Multimetastability, phototrapping, and thermal trapping of a metastable commensurate superstructure in a Fe^{II} spin-crossover compound

Sébastien Pillet,[1,*] El-Eulmi Bendeif,[1] Sylvestre Bonnet,[2] Helena J. Shepherd,[3] and Philippe Guionneau[4]

[1]*Laboratoire de Cristallographie, Résonance Magnétique et Modélisations, UMR CNRS 7036, Institut Jean Barriol, Université de Lorraine, B.P. 70239, F-54506 Vandoeuvre-lès-Nancy, France*

[2]*Leiden Institute of Chemistry, Gorlaeus Laboratories, Leiden University, P.O. Box 9502, 2300 RA Leiden, The Netherlands*

[3]*Laboratoire de Chimie de Coordination (LCC), CNRS, 205 route de Narbonne, F-31077 Toulouse, France*

[4]*CNRS, Université de Bordeaux, ICMCB, 87 Avenue du Dr A. Schweitzer, F-33608 Pessac, France*

(Received 12 April 2012; published 14 August 2012)

The photoinduced switching and subsequent relaxation regime at cryogenic temperatures of the two-step spin-crossover compound [Fe(bapbpy)$(NCS)_2$] has been investigated by time-dependent photocrystallography. Upon photoexcitation from the low-spin (LS) state, a direct population of the metastable high-spin (HS) state occurs, without involving any intermediate structural state. The relaxation from the metastable HS state in isothermal conditions at 40 K proceeds in two successive steps associated with two symmetry breaking processes. The first step corresponds to the cooperative transformation to an intermediate superstructure, characterized by a long-range-ordered [HS-LS-LS] motif coupled to a commensurate displacive modulation, and concomitant with a tripling of the c axis of the unit cell ($C2/c$ space group). The stabilization of the intermediate state is driven by strong molecule-lattice coupling. In the second stage, the intermediate state undergoes a transformation twinning triggered by lattice strain towards the LS state. The two-step relaxation is reminiscent of the two-step thermal transition of [Fe(bapbpy)$(NCS)_2$] and evidences multimetastability in the light-induced or relaxation regime. The long-range-ordered [HS-LS-LS] superstructure has also been trapped by rapid quench cooling to very low temperature, and has been structurally characterized.

DOI: 10.1103/PhysRevB.86.064106 PACS number(s): 61.50.Ks, 64.70.kt, 75.30.Wx, 31.70.Ks

I. INTRODUCTION

Spin-crossover (SCO) complexes are one of the most intensively studied molecular switchable materials;[1] their relevance in the conception of novel magnetic or optical devices presently stimulates much research effort.[2] For Fe^{II} SCO systems, the reversible switching between the high-spin (HS, $S = 2$) and the low-spin (LS, $S = 0$) molecular states is accompanied by drastic changes in optical, magnetic, and dielectric properties, and may be triggered by a variation of temperature or pressure, by guest molecule inclusion, or by light irradiation. This latter process, called LIESST[3,4] (light-induced excited spin-state trapping), consists of a conversion from the thermodynamically stable LS state to a metastable HS state with extended lifetime below the limiting temperature T(LIESST).[5] The essential characteristics of the spin transition strongly depend on the cooperativity, which results from the local structural distortion associated with the molecular spin state change (HS-LS molecular volume change in a first approximation), coupled to long-range interactions of elastic origin in the crystalline solid. These interactions are mediated by intermolecular contacts, such as hydrogen bonds, π-π contacts, and van der Waals interactions within the crystal lattice, sometimes assisted by lattice solvate molecules or counterions. Strong cooperativity favors abrupt thermal transitions, possibly of first order with a hysteresis loop, as well as HS$\rightarrow$LS nonlinear sigmoïdal relaxation curves following light-induced population of the HS metastable state.[6] The mean-field approximation may well describe most of the spin transition properties in the thermal transition (quasistatic) and LIESST (dynamic) regimes.[7,8] Short-range correlations may also compete with long-range interactions and give rise to deviation from mean-field behaviors,[9] as evidenced in some cases by distinctive long relaxation tails from the LIESST state.[10]

Although the vast majority of thermal spin transitions proceed in a single step, there has been an increasing number of two-step transitions reported for polymeric,[11–17] polynuclear,[18–24] or mononuclear SCO systems.[25–44] Such transitions result most frequently from the existence of two crystallographically (symmetrically) independent SCO Fe^{II} sites with slightly different coordination environments, leading to dissimilar transition temperatures delimiting a plateau (or shoulder), which usually occurs with an approximately equal populations of HS and LS species. Alternatively, the subtle interplay between short-range correlations and long-range interactions may be such that intermediate phases with remarkable structural topologies, characterized by well-ordered patterns of HS and LS Fe^{II} molecular species, may be stabilized in a more or less wide temperature range, providing a two-step character. Commensurate intermediate superstructures[24,30–36,40–43] or incommensurate metastable modulated structures[28,29] may thus develop, most of which result from structural symmetry breaking transitions, coupled to the spin transition itself. These intermediate superstructures may be identified using detailed temperature-dependent x-ray structure analysis; the appearance of extra Bragg superstructure reflections on the x-ray diffraction pattern is a direct signature of the development of the additional long-range order. In some cases, short-range correlations provide only a partial ordering of the HS and LS Fe^{II} entities, as recently reported for the polymeric SCO material [Fe$(NCSe)_2$(bdpp)], for which a long-range HS-LS-HS-LS chain ordering with a complete disorder between adjacent chains has been evidenced by weak planes of diffuse scattering in the intermediate phase.[15] The combination of

interactions at the origin of a two-step transition is so subtle that a change of lattice solvate,[44,45] or of counterion[30,42] may be sufficient to severely affect the transition, or even completely suppress the two-step behavior.[30,44,45]

A theoretical description of two-step transitions may be provided using Ising-like models or thermodynamic models based on one- or two-sublattice schemes. Two sublattices coupled antiferroelastically with intrasublattice ferroelastic interactions[46–49] may stabilize an ordered intermediate state, corresponding to the plateau of the two-step thermal transition and characterized by a uniform order of HS or LS state within each sublattice and opposite spin state between sublattices. On the other hand, the one-sublattice approach establishes a competition between antiferroelastic short-range interactions, favoring HS-LS neighbors, and ferroelastic long-range interactions,[50,51] or a competition between first- and second-neighbor short-range antagonistic interactions.[52] Alternatively, stepped transitions have been uncovered by a Landau expansion of the Free energy in which the totally symmetric order parameter describing the spin conversion, namely the fraction of HS species γ_{HS}, is coupled to a structural order parameter (degree of ordering of the HS and LS species, or degree of orientational disorder of a solvent lattice molecule) responsible for the long-range ordering of HS and LS molecular complexes.[53,54] According to all these theoretical schemes, the two-step behavior originates from the close interplay between the SCO molecular system and the structural degrees of freedom, i.e., the molecular distortion and the lattice strain.

Detailed experimental insights into the photoexcitation and relaxation processes in two-step transition systems are still rather scarce. In common situations, the LIESST relaxation curve, defined as the evolution of γ_{HS} as a function of temperature following photoexcitation,[5] proceeds in a single step without passing through any intermediate phase.[10,31,37,42] The corresponding isothermal relaxation curves, defined as the evolution of γ_{HS} as a function of time in isothermal condition, exhibit single-exponential behaviors, with sometimes stretched elongated tails resulting from short-range correlations.[10,42] In rare cases, a stepped LIESST relaxation[16,36,38,39,43] or stepped isothermal relaxation curves[17] have been reported and attributed to the successive relaxation of different Fe^{II} sites, although no crystallographic evidence has been provided. On the contrary, the possible stabilization of a long-range-ordered intermediate superstructure, resulting from a symmetry breaking scenario in the photoexcitation or relaxation regime, has never been reported. This is the fundamental question we address in the present study and clarify through time-dependent photocrystallography.

The mononuclear Fe^{II} SCO compound [Fe(bapbpy)$(NCS)_2$] (**1**), where bapbpy = 6,6′-bis(amino-2-pyridyl)-2,2′-bipyridine, undergoes a two-step thermal spin transition (Fig. 1), with both transition steps being first-order, and accompanied by reversible symmetry breaking crystallographic phase transitions and thermal hysteresis.[40,41,55] The crystal structure has been reported at three temperatures (295 K, 190 K, and 110 K), which correspond to the three relevant states identified from the thermomagnetic behavior. In all three thermodynamically stable states, the crystal structure may be described as supramolecular chains of *trans*-

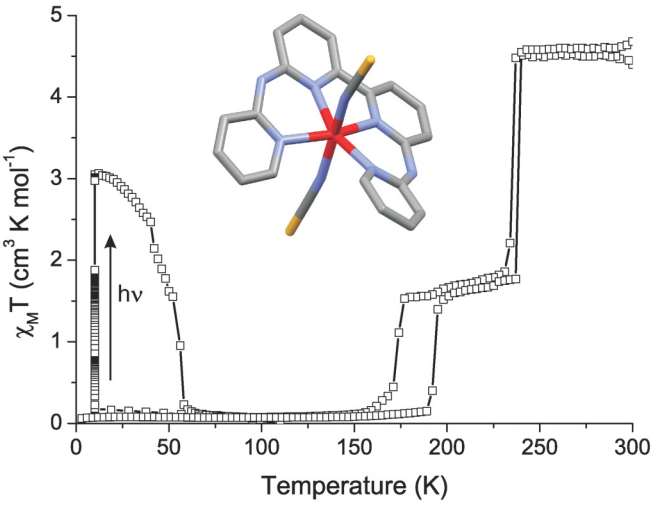

FIG. 1. (Color online) Molecular structure of **1**, and temperature dependence of the $\chi_M T$ product, showing the two-step thermal spin transition, the photoexcitation, and the subsequent relaxation (Ref. 41).

[Fe(bapbpy)$(NCS)_2$] molecules connected through N-H...S hydrogen bonds and π-π stacking interactions running along the [001] crystallographic direction. Interchain interactions in the [110] and [1$\bar{1}$0] directions are assisted by very weak C-H...S hydrogen bonds ($d_{H...S} > 2.9$ Å). State I (monoclinic $C2/c$) is observed above about 235 K and is characterized by a single HS Fe^{II} center, located on a twofold rotation axis. Cooling below this temperature leads to state II (monoclinic $C2/c$), which is characterized by a tripling of the unit cell (**a**, **b**, 3**c**), a result of the remarkable long-range order of [HS-LS-LS] spin states along [001], where the twofold symmetry is broken at the LS sites. On further cooling below about 172 K, a final transition to the fully LS state is accompanied by a decrease in the cell volume by a factor of three to form the non-merohedrally twinned state III (triclinic $C\bar{1}$),[56] which has a single crystallographically distinct LS center. The $P-T$ phase diagram of **1**, as defined from a combination of single-crystal x-ray diffraction, Raman spectroscopy, and magnetometry under hydrostatic pressures up to 16 kbar, reveals the presence of a two-step transition under pressure as well, with the same sequence of spin and crystallographic transitions.[57] Especially the crystal structure at a hydrostatic pressure of 4.6 kbar is completely isostructural with the intermediate state II determined at ambient pressure at 190 K. In addition, **1** exhibits a LIESST effect [T(LIESST) = 56 K], as evidenced by Raman spectroscopy performed at 77 K using a He-Ne excitation laser (632.8 nm), and confirmed by photomagnetic measurements.[41] Herein, we report the trapping of an ordered metastable [HS-LS-LS] superstructure for compound **1**, which is furthermore detected as an intermediate state in the two-step relaxation following LIESST, from temperature- and time-dependent x-ray crystallographic and photocrystallographic analysis.

II. CRYSTALLOGRAPHIC EXPERIMENTS

Five crystal structures, corresponding to different states with specific organizations of the molecular spin states, have

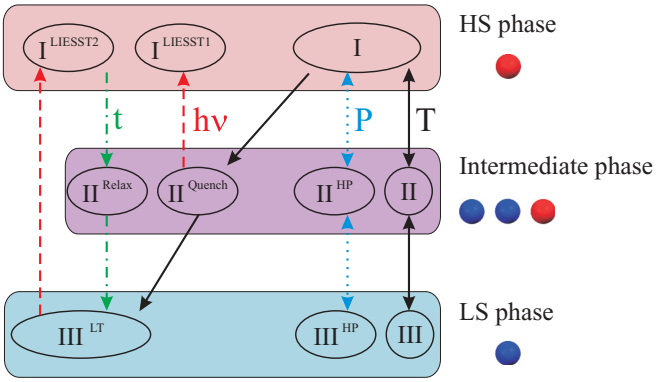

FIG. 2. (Color online) Spin state and transformation pathways between structurally characterized states in **1**. The structural states I, II, and III and the high-pressure II^{HP} and III^{HP} structural states have been reported in Refs. 40 and 57. The external stimuli triggering the spin state and state changes are temperature (T), pressure (P), and light irradiation (hν); they are depicted as continuous black, dotted blue, and dashed red arrows, respectively; time evolution (t) is shown as dashed dotted green arrows.

been determined under different procedures of temperature and/or time variation, and light irradiation conditions, as illustrated on Fig. 2. The structures are labeled II^{Quench}, III^{LT}, $I^{LIESST1}$, $I^{LIESST2}$, and II^{Relax} for the thermally quenched mixed spin state (10 K), relaxed LS state (15 K), photoinduced metastable HS state 1 (10 K), photoinduced metastable HS state 2 (15 K), and partially relaxed state after photoexcitation (15 K), respectively.

X-ray diffraction experiments were performed on single crystals using a Supernova 4-circle microsource diffractometer (Oxford Diffraction) equipped with a two-dimensional ATLAS charge-coupled-device (CCD) detector, and using Mo Kα radiation (λ = 0.71073 Å) for III^{LT}, $I^{LIESST1}$, and $I^{LIESST2}$. For II^{Quench} and II^{Relax}, Cu Kα radiation (λ = 1.54184 Å) was preferred in order to better separate superlattice reflections for these structural states with large unit cell volume. We used an Oxford Diffraction Helijet He open-flow cryosystem for cryogenic temperature measurements. For photoinduced experiments, an Ar-Kr gas laser coupled to a fiber optic (647 nm, 5mW) was used; the wavelength of the laser has been chosen after several irradiation tests and according to previously reported photomagnetic experiments.[41] Data reduction was carried out using the CrysAlis software.[58] The structures were solved by direct methods (SHELXS-97)[59] and refined against F^2 by full-matrix least squares (SHELXL-97).[60] Crystallographic details are provided in the Supplemental Material (Table S1).[61,62] Selected bond lengths, angles, and additional structural parameters discussed in the text are summarized in Table I of this paper and in Tables S2, S3, and S4 of the Supplemental Material.[62]

III. RESULTS

The structural analysis of SCO molecular crystals is very informative with respect to the spin transition process. The parameters of the Fe^{II} coordination sphere, such as bond lengths, angles, and octahedron volume V_p, are highly sensitive to the spin state; this is due to the redistribution of the valence electrons within the bonding and antibonding 3*d* orbitals of the central Fe^{II} cation upon spin-state change, as revealed from experimental electron density studies.[63] A careful inspection of these parameters allows a clear assignment of the spin state for each Fe^{II} crystallographic site. Kinetic crystallographic measurements provide qualitative and quantitative insights on the phase transformation mechanisms associated with the spin-state change. The dynamics of like-spin-domain nucleation and growth for heterogeneous cooperative transitions has indeed been determined using kinetic thermo- and photocrystallographic techniques.[64–66] In the following, we analyze successively the effect of a rapid quench cooling from room temperature to 10 K, the LS→HS photoexcitation process, and the subsequent HS→LS relaxation regime.

A. Trapping a metastable superstructure by quench cooling

At first, a single-crystal sample was rapidly quench cooled from room temperature to 10 K, and a complete x-ray diffraction data set was collected at that temperature. The resulting diffraction pattern displays superstructure reflections in addition to the main Bragg reflections, which correspond to a commensurate modulation of the crystal structure with wave vector $\mathbf{q} = 1/3\mathbf{c}^*$, or equivalently a triple unit cell (**a**, **b**, 3**c**). For consistency with the structures already reported for the thermal transition by Bonnet *et al.*,[40] the structure II^{Quench} has been solved and refined in the C-centred cell (monoclinic space group $C2/c$) with cell parameters $a = 15.7695(7)$ Å, $b = 10.6880(6)$ Å, $c = 42.313(1)$ Å, $\beta = 116.450(4)^\circ$. The I→II^{Quench} phase transition upon thermal quenching at 10 K may be described as a group-subgroup isomorphic transition, without changing the space group type ($C2/c$) but with a tripling of the unit cell volume. The overall crystal packing in the structure II^{Quench} remains similar to those derived for the thermodynamically stable state II obtained at 190 K during

TABLE I. Selected structural parameters: Average Fe-N bond length (Å), angular distortion parameter Σ (deg), and FeN_6 octahedron volume V_p (Å^3).

	II^{Quench}	II^{Relax}	III^{LT}	$I^{LIESST1}$	$I^{LIESST2}$
$d_{\langle Fe1\text{-}N\rangle}$ (Å)	1.960(4)	1.958(8)	1.955(4)	2.147(1)	2.149(1)
$d_{\langle Fe2\text{-}N\rangle}$ (Å)	2.138(4)	2.096(8)			
Σ1 (deg)	57.36	57.00	57.13	99.93	99.77
Σ2 (deg)	94.00	83.60			
$V_p(Fe1N_6)$ (Å^3)	9.91(4)	9.93(7)	9.83(4)	12.49(2)	12.53(1)
$V_p(Fe2N_6)$ (Å^3)	12.40(4)	11.88(9)			

the thermal study. The hydrogen bonds and π-π interactions along the supramolecular [001] chains (Fig. S1 in the Supplemental Material[62]) are barely significantly shorter than that characterized for state II (Tables S3 and S4). All the derived structural parameters (Table I, Table S2), especially the Fe-N bond distances [$d_{\langle Fe1\text{-}N\rangle} = 1.960(4)$ Å, $d_{\langle Fe2\text{-}N\rangle} = 2.138(4)$ Å], angular distortion parameters[67] ($\Sigma 1 = 57.36°$, $\Sigma 2 = 94.00°$), and FeN_6 octahedron volumes [$V_p(Fe1) = 9.91(4)$ Å^3, $V_p(Fe2) = 12.40(4)$ Å^3] indicate that the asymmetric unit consists of one LS molecule on a general crystallographic position (Fe1) and half of a HS molecule sitting on a twofold axis (Fe2). The structure II^{Quench} presents therefore an ordered [HS-LS-LS] motif (see Fig. S1), very similar to the structural topology of the intermediate-state II previously described by Bonnet *et al.* in their temperature variation study.[40] It is also isostructural with the intermediate state revealed at ambient temperature under hydrostatic pressure of 4.6 kbar.[57]

The self-organization of the Fe^{II} HS and LS molecules within the crystal lattice to form the [HS-LS-LS] motif is the origin of the commensurate modulation, and tripling of the unit cell in the crystallographic **c** direction. This process produces in parallel a lattice relaxation characterized by a harmonic displacive modulation of the structure with wave vector $\mathbf{q} = 1/3\mathbf{c}^*$ and transverse displacement along the direction [010]; the Fe^{II} cations are displaced by as much as 0.608 Å from the regular $y = 0$ position (Figs. 3 and 4) (the displacement is only 0.110 Å in state I at room temperature). The Fe...Fe separation distances along the supramolecular [001] chains are also modulated, the HS...LS contacts being shorter by 0.108 Å with respect to the LS...LS contacts, corresponding to longitudinal displacements (Fig. 3). This commensurate modulation of the crystal structure II^{Quench} results from a delicate coupling between spin-state ordering and displacive distortion; this coupling is expected to be quite strong in such ferroelastic materials. Since the chains are related by cell translations in the **a** and **b** directions and by the C lattice centering, corresponding to the translation symmetries $\mathbf{t} = \mathbf{a}$, $\mathbf{t} = \mathbf{b}$ and $\mathbf{t} = 1/2\mathbf{a} + 1/2\mathbf{b}$, respectively, the corrugation of adjacent chains in the packing is exactly in phase. As a consequence the modulation does not modify severely the nature and length of the weak interchain C-H...S contacts.

The trapping of a HS metastable phase at cryogenic temperature from rapid-quench-cooling a single-crystal sample is not uncommon for SCO materials.[28–30,68] To prove effectively the metastability of the thermally quenched structural state II^{Quench} in **1**, the single-crystal sample was subsequently warmed to 60 K while monitoring the unit cell volume and presence of superstructure reflections; no significant evolution was detected up to 60 K (data not shown). At 60 K, the superstructure reflection rapidly disappeared jointly with a unit cell volume contraction. This is attributed to the relaxation from the metastable state II^{Quench} to the thermodynamically stable state III. This temperature of 60 K closely matches the T(LIESST) temperature derived from the photomagnetic measurements.[41] Owing to the slow relaxation from state II to the thermodynamically stable state III in the tunnel relaxation regime at 10 K, we can therefore consider that the structure II^{Quench} corresponds to a metastable state II trapped at very low temperature.

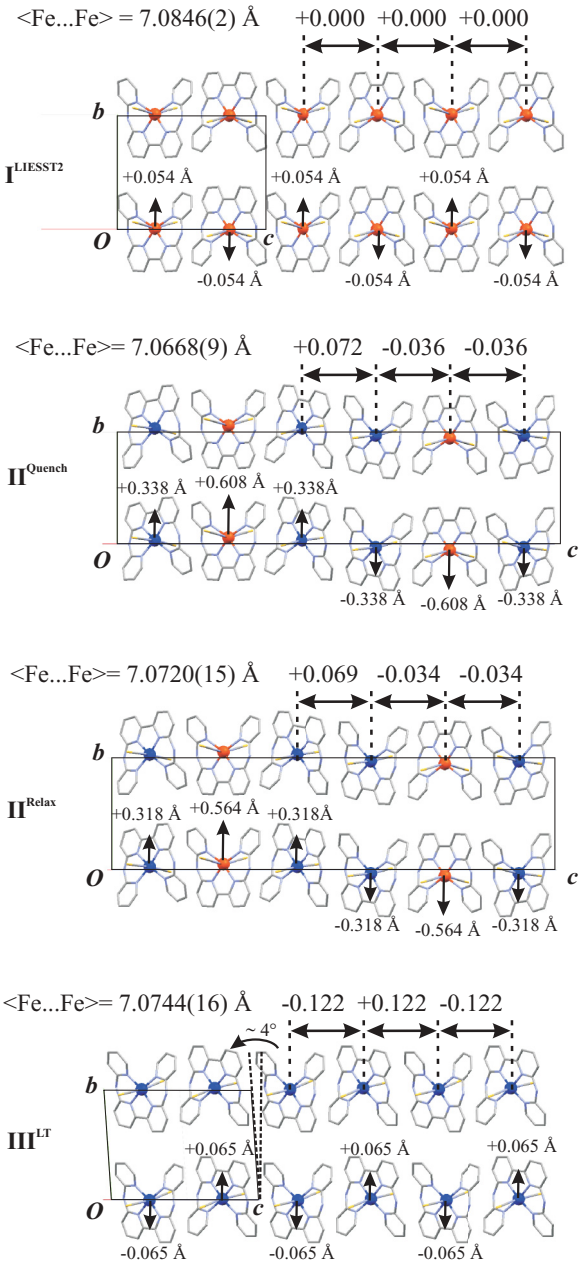

FIG. 3. (Color online) Section of the crystal packing in the (bc) plane indicating the displacement of the Fe^{II} atoms along the **b** direction from the regular $y = 0$ position, and Fe...Fe separation distances along the **c** direction with respect to the average Fe...Fe distance. HS Fe^{II} centers are shown in red, LS Fe^{II} centers in blue. Hydrogen atoms have been omitted for clarity.

The sample was then cooled from 60 K to 15 K, and a complete x-ray diffraction data set was collected. The corresponding crystal structure (labeled hereafter III^{LT}) was derived in the nonstandard space group $C\bar{1}$, with cell parameters $a = 15.7351(11)$ Å, $b = 10.5753(7)$ Å, $c = 14.1454(11)$ Å, $\alpha = 93.975(6)°$, $\beta = 116.113(7)°$, $\gamma = 90.121(6)°$. This structure is non-merohedrally twinned with the twin element being a twofold axis parallel to the crystallographic [010] direction of the C-centered cell, as reported previously for the structural analysis of state III at 110 K.[40] With respect to the structure II^{Quench}, the asymmetric unit of III^{LT} contains only one

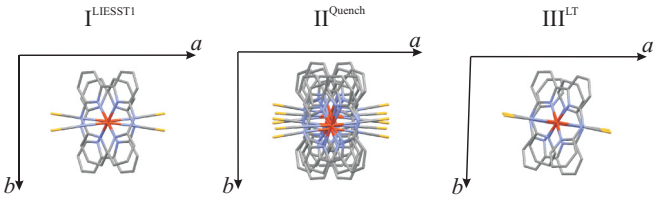

FIG. 4. (Color online) Projection of the structure of the supramolecular chain along the crystallographic **c** axis, showing the lateral corrugation of the chains in the [010] direction for structure II^{Quench}. Hydrogen atoms have been omitted for clarity.

molecule located on a general position. The $II^{Quench} \rightarrow III^{LT}$ transition is therefore associated with a symmetry breaking process. The Fe-N bond lengths [$d_{\langle Fe1\text{-}N\rangle} = 1.955(4)$ Å], iron coordination octahedron volume [$V_p = 9.83(4)$ Å^3], and angular distortion parameter ($\Sigma = 57.13^\circ$) are typical for Fe^{II} centers in the LS state (Table I) and comparable to those already reported for state III at 110 K.[40] Upon the $II^{Quench} \rightarrow III^{LT}$ structural change, the commensurate modulation is lost, as revealed by the disappearance of the superstructure reflections. The displacement of the Fe^{II} cations from the regular position $y = 0$ is reduced to 0.065 Å (Fig. 3). The supramolecular [001] chains consist of LS molecules with alternatively short and long contacts; the corresponding Fe...Fe separation distances are 6.9521(16) Å and 7.1967(16) Å.

B. Photoexcitation process and multimetastability

A fresh single-crystal sample was prepared beforehand in the II^{Quench} state at 10 K by quench cooling as described in Sec. III A, and was subsequently irradiated with an Ar-Kr gas laser (647 nm, 5mW). The crystal structure of the metastable light-induced state (labeled $I^{LIESST1}$) was derived under permanent laser irradiation. Upon the $II^{Quench} \rightarrow I^{LIESST1}$ light-induced state change, the commensurate modulation is lost, as revealed by the complete disappearance of the superstructure reflections, and the unit cell volume decreases by a factor of 3. The resulting structure contains half a molecule in the asymmetric unit in the $C2/c$ space group with cell parameters $a = 15.913(1)$ Å, $b = 10.8466(5)$ Å, $c = 14.1359(8)$ Å, $\beta = 117.211(8)^\circ$. The corresponding Fe-N coordination distances [$d_{\langle Fe1\text{-}N\rangle} = 2.147(1)$ Å], FeN_6 octahedron volume [$V_p = 12.49(2)$ Å^3], and angular distortion parameter ($\Sigma = 99.93^\circ$) indicate that the LS molecule of the state II^{Quench} has been switched to the HS state. The displacive modulation is lost, and the displacement of the Fe^{II} cations from the regular position $y = 0$ is reduced to 0.054 Å (Fig. 3). In parallel, the alternation of short Fe(LS)...Fe(HS) and long Fe(LS)...Fe(LS) contacts, which characterizes the structure II^{Quench}, disappears in structure $I^{LIESST1}$. All intramolecular and intermolecular structural parameters are very similar to those derived for state I at 295 K, taking into account thermal contraction effects.[40] Those results confirm that the displacive modulation of the structure II^{Quench} is intrinsically related to the [HS-LS-LS] spin state ordering.

Multimetastability is the ability to populate multiple metastable states with different physical (magnetic, optical, structural) properties. It has been observed for a very limited number of SCO complexes.[28,29,36,69–71] In $[Fe(bpp)_2](CF_3SO_3)_2 \cdot H_2O$ for instance, multimetastability manifests itself by two different relaxation mechanisms for the HS thermally trapped and LIESST HS states. This is possibly related to an additional structural phase transition influencing the HS→LS relaxation for the thermally trapped state.[69] Multimetastability has also been shown to occur for some mononuclear and dinuclear spin-crossover complexes undergoing two-step spin transitions. For instance, the complex $Fe(abpt)_2(N[CN]_2)_2$ exhibits two different metastable HS states at very low temperature, upon rapid thermal quenching from room temperature and upon light excitation from the LS state through the LIESST effect.[28,29] Both metastable states exhibit an incommensurate modulation of the crystal structure, with a distinct modulation wave vector: The two metastable states are structurally different without any ambiguity. The photocrystallographic investigation of the dinuclear complex $[Fe(bt)(NCS)_2]_2(bpym)$ has proved that depending on the wavelength of the photoexcitation source (i.e., 1310 nm or 800 nm), different metastable states with HS-LS or HS-HS structural configuration may be selectively populated.[70,71] As far as **1** is concerned, multimetastability is crystallographically demonstrated here since state II^{Quench} and $I^{LIESST1}$, which are observed under very different phase transformation pathways (Fig. 2), present very different structural architectures, characterized by an ordered [HS-LS-LS] motif for the former and a single HS site for the latter.

In order to explore the additional possibility of purely photoinduced multimetastability, we undertook a photoexcitation experiment on the crystal previously prepared in its thermodynamically stable LS state at 15 K, III^{LT}. The sample was irradiated with an Ar-Kr gas laser (647 nm, 5 mW); the crystal structure of the metastable light-induced state (labeled $I^{LIESST2}$) was derived under permanent laser irradiation (Fig. 2). All the corresponding structural parameters are similar to those derived for state $I^{LIESST1}$ within standard uncertainties (Table I, Table S2); hence multimetastability induced solely by light is not detected for **1**. However, an interesting additional question arises concerning the photoexcitation pathway, i.e., whether an intermediate superstructure is involved, reflecting a two-step photoexcitation process. By a careful inspection of the diffraction pattern as a function of excitation time, no superstructure reflections were identified during photoexcitation (at least with the time resolution of the diffraction experiment), which indicates that the light-induced phase transition proceeds in a direct manner, avoiding any intermediate ordered metastable state. It is noteworthy that the implication of such a putative intermediate structural state has never been observed experimentally and reported in the literature.

C. Two-step relaxation

The photomagnetic measurements performed on a polycrystalline sample by Bonnet *et al.* show "a singularity in the relaxation curve around 40 K, which might indicate a two-step relaxation process," as shown in Fig. 1.[41] The multimetastability demonstrated by the present crystallographic investigations (i.e., structures II^{Quench}, $I^{LIESST1}$, and $I^{LIESST2}$) renders the hypothesis of a two-step relaxation indeed conceivable. To explore this possibility, we followed the evolution of the diffraction pattern after photoexcitation to the $I^{LIESST2}$ state

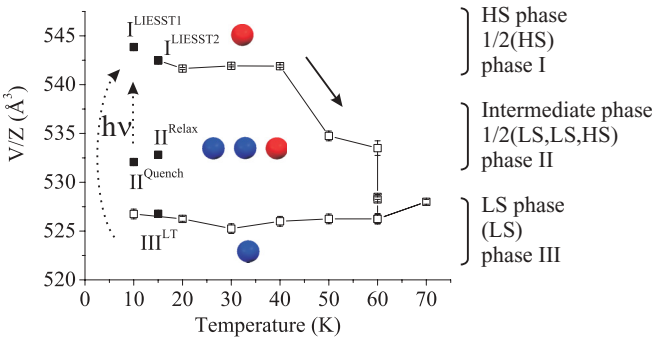

FIG. 5. (Color online) Temperature dependence of V/Z (the volume per formula unit) in the various states (empty squares). Filled squares correspond to structure determination (Table S1 in the Supplemental Material[62]).

in two ways: (i) while gradually raising the temperature from 10 K to 70 K (Fig. 5), and (ii) as a function of time in isothermal condition at 40 K (Fig. 6).

(i) While gradually increasing the temperature from 10 to 70 K in the $I^{LIESST2}$ state, no significant evolution of the unit cell volume is observed up to 40 K. At 50 K, the diffraction pattern suddenly displays superstructure reflections, related to the tripling of the unit cell (**a**, **b**, 3**c**), while the unit cell volume per formula unit (V/Z) decreases to 534.7(5) Å^3. This value matches the unit cell volume per formula unit of the structure II^{Quench} quite closely [$V/Z = 532.1(1)$ Å^3]. After this initial drop, the unit cell volume is almost constant up to 60 K and then finally decreases to a value corresponding to state III. In parallel, the superstructure reflections disappear. This singularity in the evolution of the unit cell while increasing the temperature is in good agreement with the T(LIESST) value of 55 K, and demonstrates a two-step structural relaxation process, related to the transient stabilization of an intermediate structural state.

(ii) The relaxation process has also been investigated from the evolution of the unit cell parameters and diffraction pattern as a function of time in isothermal conditions at 40 K,

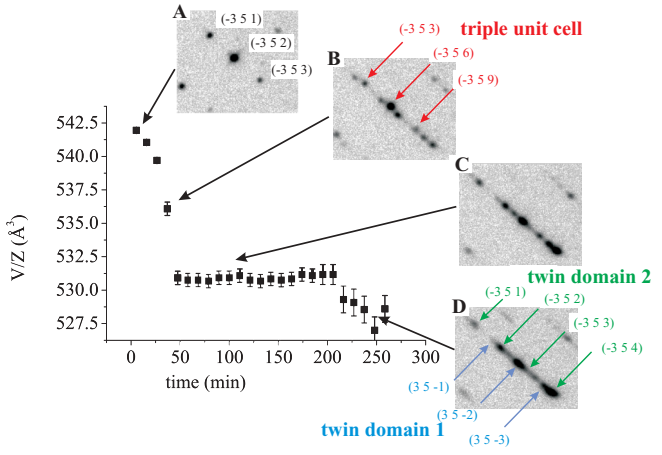

FIG. 6. (Color online) Evolution of the unit cell volume per formula unit (V/Z) during the isothermal relaxation at 40 K from the photoinduced metastable state $I^{LIESST2}$, and selected region of the diffraction pattern centered on the [−3 5 l] row.

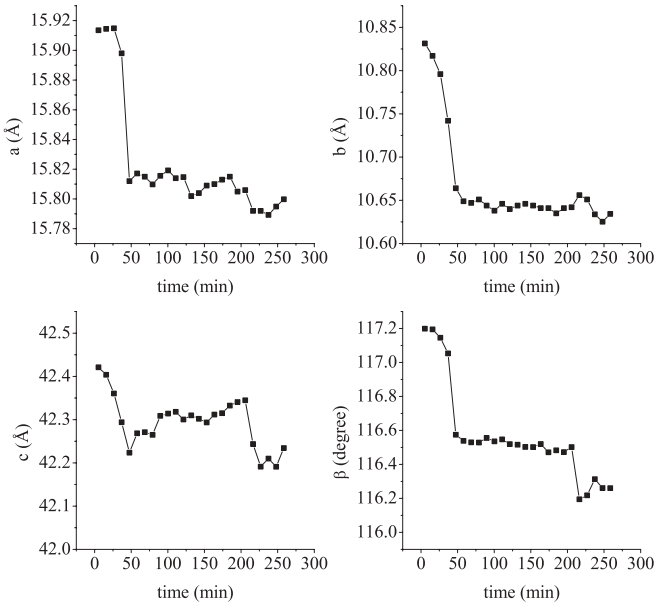

FIG. 7. Evolution of the unit cell parameters during the isothermal relaxation at 40 K from the photoinduced metastable state $I^{LIESST2}$. The **c** axes for states $I^{LIESST2}$ and III were multiplied by a factor of 3 for ease of comparison with state II^{Relax}.

allowing picturing a complete scenario of the structural phase transformation $I^{LIESST2} \rightarrow$ III; three consecutive stages may be identified (Fig. 6).

In the early step (within 50 min), a rapid and nonlinear decrease of the unit cell volume per formula unit occurs. Superstructure reflections, which can be indexed with the commensurate wave vector $\mathbf{q} = 1/3\mathbf{c}^*$, progressively develop, indicating the growth of a superstructure intermediate state (structure labeled II^{Relax}). The sigmoidal trend of the unit cell evolution indicates that this state transformation takes place in a cooperative manner. As detailed in Fig. 7, the evolution of the unit cell parameters is anisotropic during this first period, the crystallographic **b** axis shortens progressively by about 1.7%, while the **a** and **c** axes decrease by 0.6% and 0.4% respectively, which is the reason for the unit cell volume contraction. The intensity profile along the [−3 5 l] row as a function of time (Fig. 8) clearly shows that the superstructure reflections may be detected around $t = 37$ min [see reflection (−3 5 7) for instance]—that is to say, well after the contraction of the crystallographic **b** axis started. At this point, the intensity of the superstructure reflections is almost 1/3 of their intensity at the end of stage 1 (Fig. 9). The intensity of the (−3 5 6) reflection decreases almost to zero during the first step of the transformation (from $t = 0$ to $t = 50$ min), and as such, it may be taken as a signature of the disappearance of the state $I^{LIESST2}$.

In the second step, the unit cell volume is constant over a period of 150 min, during which a large modification of the diffraction pattern occurs. It is noteworthy that the cell parameters do not change significantly during this period, with the exception of a gradual slight increase of the **c** axis. However, the diffraction pattern still evolves drastically (Fig. 6), as well as the intensity of some of the superstructure reflections, revealing that the phase transformation is still proceeding,

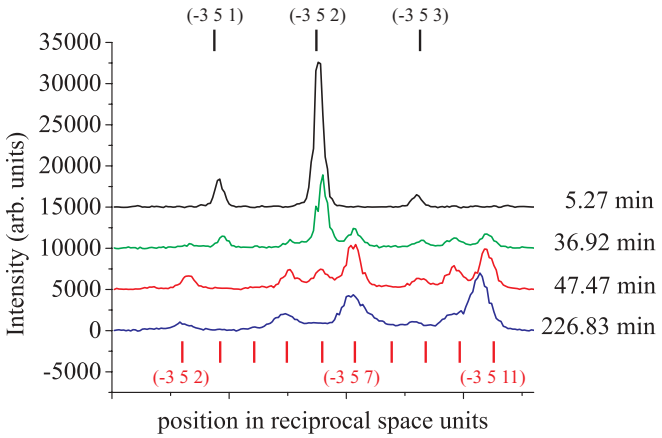

FIG. 8. (Color online) Intensity profile along the [−3 5 *l*] row during the relaxation at 40 K from the photoinduced metastable state $I^{LIESST2}$, corresponding to the selected regions of reciprocal space depicted in Fig. 6. The profiles have been displaced vertically for clarity. Vertical black and red ticks define the position of the diffraction peaks with respect to the primitive C-centered cell of structure III^{LT} and triple C-centered cell of structure II^{Relax}, respectively. For instance, the (−3 5 2) reflection indexed with respect to the reduced C-centered cell corresponds to (−3 5 6) in the triple C-centered cell indexing.

albeit at constant unit cell volume. From $t = 58$ min, the intensity of the reflection (−3 5 7) gradually decreases, which is a clear indication that a structural transformation is indeed developing on the plateau. We consider that twin domains are progressively formed throughout the crystal during this period. On the contrary, the (−3 5 11) reflection is completely insensitive to the twin formation as its intensity is not changing significantly after the first rapid increase to $t = 58$ min. At $t \approx 215$ min, the unit cell parameters **c** and β, and to a lower extent **a**, present an abrupt decrease, and consequently the unit cell volume reduces, corresponding most probably to the final $II^{Relax} \rightarrow III$ phase transition.

One fundamental question is whether the intermediate modulated state II^{Relax} observed during the isothermal relaxation at 40 K exhibits a superstructure with an ordered pattern of HS and LS species, similar to the structures II, II^{Quench}, and II^{HP}. Unfortunately, the crystal structure of the modulated intermediate state II^{Relax} could not be derived experimentally from the previous crystallographic measurement at 40 K. Indeed, thermal fluctuations are strong enough at this temperature to overcome the energy barrier to relaxation to the LS state, leading to a limited lifetime of the II^{Relax} state at 40 K. Accordingly, the two-step isothermal relaxation was repeated at 40 K on a fresh crystal, monitoring carefully the evolution of the unit cell volume and appearance of the superstructure reflections as a function of time. Once the single-crystal sample reached the intermediate plateau, the temperature of the cryosystem was decreased rapidly to 15 K to decrease as much as possible the effect of thermal fluctuations, and thus increase sufficiently the lifetime of the II^{Relax} state to enable a structural determination. A complete diffraction data collection was performed, and the corresponding crystal structure II^{Relax} was derived. It is important to stress that this procedure is very delicate. Obviously, the quality of the corresponding diffraction data is lower than for all the other crystal structures we derived in the present work, since the crystal suffered significant damage owing to the sequence of phase transitions it underwent before reaching the final point at which the data collection was performed. Correlatively, the internal agreement factor of the data collection (R_{int}) and the agreement factors of the least-squares structural refinement [$R(F^2)$ and $wR(F^2)$] are significantly higher than for all the other crystal structures. However, we consider that this structural analysis is relevant and accurate enough for getting decisive structural information on the relaxation mechanism. As given in Table I (and Table S2), the coordination environment of Fe1 in state II^{Relax} is very similar to those derived for Fe1 in state II^{Quench}, while Fe2 exhibits average Fe-N coordination distances, Σ angular distortion parameter, and FeN_6 octahedron volume close to but slightly lower than those expected for a genuine HS Fe^{II} environment. This may be attributed to the difficulty in efficiently trapping the crystal in the II^{Relax} state using our experimental procedure. It is therefore convincing that the II^{Relax} crystal structure exhibits the same [HS-LS-LS] superstructure as in all other stable or metastable structures of state II. The transverse displacements of the two Fe^{II} cations from the regular $y = 0$ position amounts to 0.318 Å and 0.564 Å for Fe1 and Fe2, respectively, under the effect of the displacive modulation concomitant with the [HS-LS-LS] spin state ordering. These values are close to those derived for the structure II^{Quench}, which gives strong evidence that the step in the relaxation process is related to the stabilization of an ordered [HS-LS-LS] superstructure.

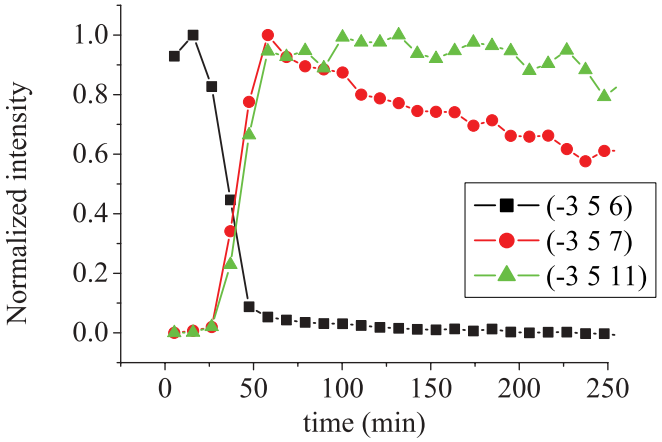

FIG. 9. (Color online) Normalized intensity variation of the (−3 5 6), (−3 5 7), and (−3 5 11) diffraction peaks as a function of time during the isothermal relaxation at 40 K. The indexing of the three diffraction peaks refers to the triple C-centered cell of state II^{Relax}.

IV. DISCUSSION

We have shown through our crystallographic analysis that the LIESST relaxation in **1** occurs in two successive steps with an intermediate plateau, which manifests itself in the relaxation while raising the temperature, and as a function of time in isothermal condition. This is an outstanding behavior that deserves additional comments. The two-step relaxation involves the sequence of states $I^{LIESST2} \rightarrow II^{Relax} \rightarrow III$. The first step of the transformation is associated with the development

of a commensurate modulated superstructure, during which the unit cell triples (**a**, **b**, 3**c**) and the point group symmetry $2/m$ is preserved. It may be described as a group-subgroup isomorphic transition, without changing the space group type ($C2/c$). The stabilization of the intermediate superstructure state reveals a structural instability originating from a strong coupling between lattice distortions (spontaneous strain) and molecular spin state change. It leads to a displacive modulation of the structure with wave vector $\mathbf{q} = 1/3\mathbf{c}^*$ and large displacement amplitudes (up to 0.564 Å). The second step is associated with a symmetry breaking from state $\mathrm{II}^{\mathrm{Relax}}$ to the lower symmetry structure of state III, the twofold axis is lost, the point group symmetry decreases to -1, and the unit cell volume is divided by 3. Accordingly, the sequence of phase transition $\mathrm{I}^{\mathrm{LIESST2}} \rightarrow \mathrm{II}^{\mathrm{Relax}} \rightarrow \mathrm{III}$ does not belong to the reentrant situation. The two steps of the transformation generate large elastic strain, which has also been observed during the thermal transition by polarized light measurements.[55] Especially during the second step $\mathrm{II}^{\mathrm{Relax}} \rightarrow \mathrm{III}$, the crystal lattice distorts appreciably as reflected by the deviation of the angle α ($\alpha \approx 94^\circ$) from the monoclinic value ($\alpha = 90^\circ$), while the angle γ does not deviate so strongly [$\gamma = 90.121(6)^\circ$]. In order to accommodate the corresponding change in structure and the associated strain, the crystal adopts a collective response and tends to develop transformation twins. The twofold symmetry axis which is lost during the symmetry breaking transition relates the individual twin components; the associated composition plane is the (**ab**) plane of the triclinic crystal (Fig. S2). This is consistent with the optical microscopy observations during the thermal transition $\mathrm{II} \rightarrow \mathrm{III}$, which revealed a homogeneous domain pattern characterized by micrometric stripes with domain walls of parallel orientations (lamellar twin) perpendicular to the crystallographic **c** axis.[55] This is a quite common twin domain pattern for ferroelastic materials.[72] The twin formation results in a close-to-zero net spontaneous strain as a result of mutual cancellation; the elastic energy has to be minimized on a mesoscopic scale; this is the driving force for the twin formation.[72]

Two-step relaxation following LIESST is very uncommon in SCO materials. It has been reported for just a few systems,[16,17,36,38,39,43] but it has never been characterized and successfully interpreted on the basis of the underlying evolution of the crystal structure. The most trivial situation is that of several crystallographic Fe^{II} sites in the metastable HS state, in which case the several steps of the relaxation are associated with the successive, and not concomitant, relaxation of the different sites owing to different lifetime of the metastable HS molecular species. For $[\mathrm{Fe(DPEA)(bim)}](\mathrm{ClO_4})_2 \cdot 0.5\mathrm{H_2O}$, two LIESST relaxation temperatures have been detected in the $\partial(\chi_M T)/\partial T$ versus T plot by photomagnetic measurements (viz., 21 K and 36 K) and assigned to the two Fe^{II} sites having different T(LIESST) values.[38] The same situation holds for $[\mathrm{Fe(picpzpz)_2}](\mathrm{BF_4})_2 \cdot \mathrm{MeOH}$ with the two relaxation temperatures being 49 K and 70 K.[39] On the contrary, the isothermal relaxation at 10 K for this former compound did not evidence any two-step character, but rather a stretched exponential behavior, which has been well adjusted to a biexponential relaxation law. The same situation has been reported for the fascinating SCO material $\mathrm{Fe(dpp)_2[Ni(mnt)_2]_2} \cdot \mathrm{MeOH}$, whose thermal spin transition exhibits three intermediate states. One of these states (labeled state IM1 in Ref. 36) corresponds to a superstructure in a tripled unit cell with 1/3 Fe^{II} in the HS state and 2/3 Fe^{II} in the LS state. Interestingly, the magnetic and photomagnetic measurements indicate that the trapped HS state relaxes to the LS state in two steps with a $\chi_M T$ value at the intermediate plateau which is close to those of the IM1 state. This suggests that the two-step relaxation proceeds through the intermediate IM1 state, although no crystallographic results have been provided by the authors to confirm this important issue. The $\mathrm{HS} \rightarrow \mathrm{LS}$ relaxation kinetics of the SCO coordination polymer $\mathrm{Fe(pmd)[Ag(CN)_2][Ag_2(CN)_3]}$ has been investigated in detail by optical spectroscopy as a function of temperature between 15 and 55 K.[17] The derived isothermal relaxation takes place via a two-step cooperative process, which has been attributed to the successive individual relaxation of the five independent Fe^{II} sites. The two-site (or two groups of sites) explanation for those two-step relaxations is relevant since it is well known that T(LIESST) is primarily governed by the geometry of the inner coordination sphere and conformational rigidity of the coordinating ligands, while the intermolecular interactions in the crystal packing are supposed to have a minor influence.[5] However, in several other SCO systems with two-step thermal transitions, LIESST relaxation proceeds in a single step without passing through any intermediate state.[10,31,37,42] In such cases, one single T(LIESST) relaxation temperature is characterized, while the relaxation kinetics can be adequately described by a single sigmoidal law or a stretched exponential. The SCO mononuclear system $[\mathrm{Fe(pic)_3}]\mathrm{Cl_2} \cdot \mathrm{EtOH}$ is the most well known representative example of these. It exhibits a two-step thermal spin transition coupled to a symmetry breaking phenomenon which leads to an ordered superstructure on the plateau.[35] The $\mathrm{HS} \rightarrow \mathrm{LS}$ relaxation following LIESST at cryogenic temperature exhibits the typical sigmoidal behavior with stretched elongated tails resulting from short-range correlations.[10] The two-site explanation for a two-step relaxation does not hold for **1** since the crystal structure of the $\mathrm{I}^{\mathrm{LIESST1}}$ and $\mathrm{I}^{\mathrm{LIESST2}}$ states evidences only one symmetrically independent HS site. On the contrary, the crystallographic analysis reveals that the $\mathrm{HS} \rightarrow \mathrm{LS}$ relaxation is associated with a double symmetry breaking phenomenon with the stabilization of an intermediate superstructure state $\mathrm{II}^{\mathrm{Relax}}$. To the best of our knowledge, **1** is the first example of a SCO compound exhibiting such a two-step relaxation process that has been elucidated crystallographically.

In the dynamic regime, two-step relaxations may well be interpreted on the basis of Ising-like models with antagonistic interactions between two coupled sublattices,[48,50,73,74] or alternatively considering antiferroelastic short-range interactions balanced by ferroelastic long-range interactions without introducing two sublattices.[10] In all these schemes, the intermediate state results from an instability originating from the competing interactions or competing sublattices, leading in some cases to an ordered pattern of HS and LS species (i.e., a superstructure).[74] Two regimes in the relaxation curves may emerge for strong enough antiferroelastic intersublattice interactions.[73] It is noteworthy that these interactions control the width of the plateau at the two-step thermal transition as well; the width has been shown to depend linearly on the value of the intersublattice coupling constant.[48,73] As shown

in Ref. 48, the delicate interplay between intrasublattice and intersublattice plays a fundamental role in the metastability and lifetime of the HS and intermediate states, so that 1 step, 2 step, or 1 step relaxations with trapping to the intermediate state can occur as a function of temperature. As far as **1** is concerned, the two-step thermal transition with a HS to LS population ratio of 1/3 on the plateau has been uncovered using an Ising-like model with three interacting sublattices.[41,57] The width of the thermal transition plateau is quite large for **1** (50 K), and the two steps are associated with hysteresis behaviors, which confirm that indeed the intersublattice coupling might be strong in this material. Following the arguments of the dynamic Ising-like models discussed above, it is therefore not unexpected that a two-step relaxation process occurs in the dynamic regime at cryogenic temperature. It has been shown that theoretically, the lifetime of the intermediate state should be strongly dependent on temperature due to the competition between thermal fluctuations and the energy barrier to the relaxation into the equilibrium LS state.[48] Experimentally, the two-step relaxation in **1** has been probed and structurally characterized at 40 K, that is to say, close to T(LIESST). Such a two-step relaxation associated with a symmetry breaking transition has been predicted to occur for strong intersublattice interactions[75] while raising the temperature under continuous light irradiation in the so-called LITH regime (light-induced thermal hysteresis), i.e., close to T(LIESST).

Figure 2 summarizes all the states of **1** that have been structurally characterized from crystallography as a function of temperature, pressure, and light irradiation. It also shows the transformation pathways relating these states. It is noteworthy that some of the transformation pathways are reversible, while some are completely irreversible (I→II$^{\text{Quench}}$ for instance). It is also remarkable that the superstructure with ordered [HS-LS-LS] motif is involved as an intermediate state in almost all the I↔III phase transformations, the only exception being the I→III light-induced transition. This is not surprising since photoexcitation is intrinsically a random process, which breaks short-range correlations.[9] The build-up of such correlations would be crucial for the development of an ordered intermediate superstructure. Photoexcitation curves reporting the evolution of the HS fraction γ_{HS} as a function of time at very low temperature under continuous laser light irradiation are only rarely reported, and do not exhibit 2-step photoexcitation in general.[42] As predicted by Parreira *et al.*, a two-step photoinduced transition passing through a symmetry breaking intermediate state may occur in the LITH regime.[75]

V. CONCLUSION

In summary, the light-induced excitation and subsequent relaxation regime at cryogenic temperature of the two-step SCO complex [Fe(bapbpy)$(NCS)_2$] have been investigated by time-dependent photocrystallography. Upon photoexcitation from the totally LS phase (structure III$^{\text{LT}}$), a direct population of the totally HS phase (structure I$^{\text{LIESST2}}$) occurs, without involving any intermediate structural phase. The relaxation from the metastable state I$^{\text{LIESST2}}$ at 40 K proceeds in two steps. The first step corresponds to the cooperative transformation to an intermediate superstructure II$^{\text{Relax}}$ characterized by a long-range-ordered [HS-LS-LS] motif coupled to a commensurate displacive modulation. In a second stage, state II$^{\text{Relax}}$ undergoes a transformation twinning towards the LS state III, triggered by lattice strain. The formation of the superstructure is driven by strong molecule-lattice coupling, and results from the subtle interplay between short-range interactions and ferroelastic long-range interactions along the supramolecular chains. The long-range-ordered [HS-LS-LS] superstructure has also been trapped as II$^{\text{Quench}}$ by rapid thermal quenching of state I to cryogenic temperature. **1** exhibits therefore multimetastability (states I$^{\text{LIESST1}}$, I$^{\text{LIESST2}}$, II$^{\text{Relax}}$, II$^{\text{Quench}}$), which has been completely characterized structurally. This property of multimetastability is of the utmost importance, paving the way for the development of innovative multiswitchable molecular systems. To the best of our knowledge, **1** is the first example of a SCO compound exhibiting such a two-step relaxation related to a double symmetry breaking process to have been elucidated crystallographically.

ACKNOWLEDGMENTS

This work was supported by the project CROSS-NANOMAT (ANR-10-BLAN-0716), the Université de Lorraine, the CNRS, and the French Ministry of Research (PPF "Cristallographie et Photocristallographie à haute résolution"). The Service Commun de Diffraction X (Université de Lorraine) is acknowledged for providing access to crystallographic facilities.

*Corresponding author; sebastien.pillet@crm2.uhp-nancy.fr

[1] P. Gütlich and H. A. Goodwin, eds., *Topics in Current Chemistry* (Springer-Verlag, Berlin, 2004), pp. 233–235.
[2] A. Bousseksou, G. Molnar, L. Salmon, and W. Nicolazzi, Chem. Soc. Rev. **40**, 3313 (2011).
[3] S. Decurtins, P. Gütlich, C. P. Köhler, and H. Spiering, Chem. Phys. Lett. **105**, 1 (1984).
[4] S. Decurtins, P. Gütlich, K. M. Hasselbach, H. Spiering, and A. Hauser, Inorg. Chem. **24**, 2174 (1985).
[5] J.-F. Létard, J. Mater. Chem. **16**, 2550 (2006).
[6] A. Hauser, P. Gütlich, and H. Spiering, Inorg. Chem. **25**, 4245 (1986).
[7] A. Hauser, Chem. Phys. Lett. **192**, 65 (1992).
[8] A. Hauser, Top. Curr. Chem. **234**, 155 (2004).
[9] H. Spiering, T. Kohlhaas, H. Romstedt, A. Hauser, C. Bruns-Yilmaz, J. Kusz, and P. Gütlich, Coord. Chem. Rev. **190–192**, 629 (1999).
[10] H. Romstedt, A. Hauser, and H. Spiering, J. Phys. Chem. Solids **59**, 265 (1998).
[11] Y. Garcia, O. Kahn, L. Rabardel, B. Chansou, L. Salmon, and J. P. Tuchagues, Inorg. Chem. **38**, 4663 (1999).
[12] C. M. Grunert, J. Schweifer, P. Weinberger, W. Linert, K. Mereiter, G. Hilscher, M. Muller, G. Wiesinger, and P. J. van Koningsbruggen, Inorg. Chem. **43**, 155 (2004).

[13]M. Carmen Munoz, A. B. Gaspar, A. Galet, and J. A. Real, Inorg. Chem. **46**, 8182 (2007).
[14]G. J. Halder, K. W. Chapman, S. M. Neville, B. Moubaraki, K. S. Murray, J.-F. Létard, and C. J. Kepert, J. Am. Chem. Soc. **130**, 17552 (2008).
[15]S. M. Neville, B. A. Leita, G. J. Halder, C. J. Kepert, B. Moubaraki, J.-F. Létard, and K. S. Murray, Chem. Eur. J. **14**, 10123 (2008).
[16]J. A. Rodriguez-Velamazan, C. Carbonera, M. Castro, E. Palacios, T. Kitazawa, J.-F. Létard, and R. Burriel, Chem. Eur. J. **16**, 8785 (2010).
[17]V. Niel, A. L. Thompson, A. E. Goeta, C. Enachescu, A. Hauser, A. Galet, M. C. Munoz, and J. A. Real, Chem. Eur. J. **11**, 2047 (2005).
[18]J. A. Real, H. Bolvin, A. Bousseksou, A. Dworkin, O. Kahn, F. Varret, and J. Zarembowitch, J. Am. Chem. Soc. **114**, 4650 (1992).
[19]J. J. M. Amoore, C. J. Kepert, J. D. Cashion, B. Moubaraki, S. M. Neville, and K. S. Murray, Chem. Eur. J. **12**, 8220 (2006).
[20]C. J. Schneider, J. D. Cashion, B. Moubaraki, S. M. Neville, S. R. Batten, D. R. Turner, and K. S. Murray, Polyhedron **26**, 1764 (2007).
[21]A. Y. Verat, N. Ould-Moussa, E. Jeanneau, B. Le Guennic, A. Bousseksou, S. A. Borshch, and G. S. Matouzenko, Chem. Eur. J. **15**, 10070 (2009).
[22]D. Y. Wu, O. Sato, Y. Einaga, and C.-Y. Duan, Angew. Chem. Int. Ed. **48**, 1475 (2009).
[23]M. Nihei, M. Ui, M. Yokota, L. Han, A. Maeda, H. Kishida, H. Okamoto, and H. Oshio, Angew. Chem. Int. Ed. **44**, 6484 (2005).
[24]K. Nakano, S. Kawata, K. Yoneda, A. Fuyuhiro, T. Yagi, S. Nasu, S. Moritomo, and S. Kaizaki, Chem. Commun. **2004**, 2892.
[25]G. S. Matouzenko, D. Luneau, G. Molnar, N. Ould-Moussa, S. Zein, S. A. Borshch, A. Bousseksou, and F. Averseng, Eur. J. Inorg. Chem. **2006**, 2671.
[26]N. Moliner, A. B. Gaspar, M. C. Munoz, V. Niel, J. Cano, and J. A. Real, Inorg. Chem. **40**, 3986 (2001).
[27]J. Klingele, D. Kaase, M. H. Klingele, J. Lach, and S. Demeshko, Dalton Trans. **39**, 1689 (2010).
[28]C. F. Sheu, S. Pillet, Y.-C. Lin, S.-M. Chen, I.-J. Hsu, C. Lecomte, and Y. Wang, Inorg. Chem. **47**, 10866 (2008).
[29]S. Pillet, C. Lecomte, C.-F. Sheu, Y.-C. Lin, I.-J. Hsu, and Y. Wang, J. Phys. Conf. Ser. **21**, 221 (2005).
[30]M. Yamada, H. Hagiwara, H. Torigoe, N. Matsumoto, M. Kojima, F. Dahan, J.-P. Tuchagues, N. Re, and S. Iijima, Chem. Eur. J. **12**, 4536 (2006).
[31]M. Buron-Le Cointe, N. Ould Moussa, E. Trzop, A. Moréac, G. Molnar, L. Toupet, A. Bousseksou, J.-F. Letard, and G. S. Matouzenko, Phys. Rev. B **82**, 214106 (2010).
[32]M. Griffin, S. Shakespeare, H. J. Shepherd, C. J. Harding, J.-F. Létard, C. Desplanches, A. E. Goeta, J. A. K. Howard, A. K. Powell, V. Mereacre, Y. Garcia, A. D. Naik, H. Müller-Bunz, and G. G. Morgan, Angew. Chem. Int. Ed. **50**, 896 (2011).
[33]N. Bréfuel, H. Watanabe, L. Toupet, J. Come, N. Matsumoto, E. Collet, K. Tanaka, and J. P. Tuchagues, Angew. Chem. Int. Ed. **48**, 9304 (2009).
[34]D. Boinnard, A. Bousseksou, A. Dworkin, J.-M. Savariault, F. Varret, and J. P. Tuchagues, Inorg. Chem. **33**, 271 (1994).
[35]D. Chernyshov, M. Hostettler, K. W. Törnroos, and H.-B. Bürgi, Angew. Chem. Int. Ed. **42**, 3825 (2003).
[36]M. Nihei, H. Tahira, N. Takahashi, Y. Otake, Y. Yamamura, K. Saito, and H. Oshio, J. Am. Chem. Soc. **132**, 3553 (2010).
[37]V. A. Money, C. Carbonera, J. Elhaïk, M. A. Halcrow, J. A. K. Howard, and J.-F. Létard, Chem. Eur. J. **13**, 5503 (2007).
[38]G. S. Matouzenko, J.-F. Létard, S. Lecocq, A. Bousseksou, L. Capes, L. Salmon, M. Perrin, O. Kahn, and A. Collet, Eur. J. Inorg. Chem. **2001**, 2935.
[39]B. A. Leita, S. M. Neville, G. J. Halder, B. Moubaraki, C. J. Kepert, J.-F. Létard, and K. S. Murray, Inorg. Chem. **46**, 8784 (2007).
[40]S. Bonnet, M. A. Siegler, J. S. Costa, G. Molnar, A. Bousseksou, A. L. Spek, P. Gamez, and J. Reedijk, Chem. Commun. **2008**, 5619.
[41]S. Bonnet, G. Molnar, J. S. Costa, M. A. Siegler, A. L. Spek, A. Bousseksou, W.-T. Fu, P. Gamez, and J. Reedijk, Chem. Mater. **21**, 1123 (2009).
[42]M. Yamada, M. Ooidemizu, Y. Ikuta, S. Osa, N. Matsumoto, S. Iijima, M. Kojima, F. Dahan, and J.-P. Tuchagues, Inorg. Chem. **42**, 8406 (2003).
[43]N. Bréfuel, E. Collet, H. Watanabe, M. Kijoma, N. Matsumoto, L. Toupet, K. Tanaka, and J.-P. Tuchagues, Chem. Eur. J. **16**, 14060 (2010).
[44]B. Li, R.-J. Wei, J. Tao, R.-B. Huang, L.-S. Zheng, and Z. Zheng, J. Am. Chem. Soc. **132**, 1558 (2010).
[45]D. Chernyshov, B. Vangdal, K. W. Törnroos, and H.-B. Bürgi, New J. Chem. **33**, 1277 (2009).
[46]A. Bousseksou, J. Nasser, J. Linares, K. Boukheddaden, and F. Varret, J. Phys. I (Paris) **2**, 1381 (1992).
[47]N. Sasaki and T. Kambara, Phys. Rev. B **40**, 2442 (1989).
[48]M. Nishino, K. Boukheddaden, S. Miyashita, and F. Varret, Phys. Rev. B **68**, 224402 (2003).
[49]T. Luty and K. Yonemitsu, J. Phys. Soc. Jpn. **73**, 1237 (2004).
[50]K. Boukheddaden, J. Linares, H. Spiering, and F. Varret, Eur. Phys. J. B **15**, 317 (2000).
[51]H. Romstedt, H. Spiering, and P. Gütlich, J. Phys. Chem. Solids **59**, 1353 (1998).
[52]K. Boukheddaden, J. Linares, R. Tanasa, and C. Chong, J. Phys.: Condens. Matter **19**, 106201 (2007).
[53]D. Chernyshov, H.-B. Bürgi, M. Hostettler, and K. W. Törnroos, Phys. Rev. B **70**, 094116 (2004).
[54]K. W. Törnroos, M. Hostettler, D. Chernyshov, B. Vangdal, and H.-B. Bürgi, Chem. Eur. J. **12**, 6207 (2006).
[55]S. Bedoui, G. Molnar, S. Bonnet, C. Quintero, H. J. Shepherd, W. Nicolazzi, L. Salmon, and A. Bousseksou, Chem. Phys. Lett. **499**, 94 (2010).
[56]The structure of state III is described in the nonconventional triclinic space group $C\bar{1}$ to preserve the orientation of the unit cell axis with respect to state I and state II, and thus facilitate the structural analysis and discussion.
[57]H. J. Shepherd, S. Bonnet, P. Guionneau, S. Bedoui, G. Garbarino, W. Nicolazzi, A. Bousseksou, and G. Molnar, Phys. Rev. B **84**, 144107 (2011).
[58]CrysAlis CCD and CrysAlis RED, version 1.171, Oxford Diffraction, Wroclaw, Poland, 2004.
[59]G. M. Sheldrick, SHELXS97, Program for Structure Solution, University of Göttingen, Göttingen, Germany, 1997.
[60]G. M. Sheldrick, SHELXL97, Program for Structure Refinement, University of Göttingen, Göttingen, Germany, 1997.
[61]CCDC-874130 to CCDC-874134 contain the supplementary crystallographic data for this paper. These data can be obtained free of charge via [http://www.ccdc.cam.ac.uk/conts/retrieving.html] or from the Cambridge Crystallographic Data Centre, 12 Union Road, Cambridge CB21EZ, UK; fax: (+44) 1223-336033; or [deposit@ccdc.cam.uk].

[62]See Supplemental Material at http://link.aps.org/supplemental/10.1103/PhysRevB.86.064106 for crystallographic details.
[63]V. Legrand, S. Pillet, M. Souhassou, N. Lugan, and C. Lecomte, J. Am. Chem. Soc. **128**, 13921 (2008).
[64]S. Pillet, J. Hubsch, and C. Lecomte, Eur. Phys. J. B **38**, 541 (2004).
[65]S. Pillet, V. Legrand, M. Souhassou, and C. Lecomte, Phys. Rev. B **74**, 140101 (2006).
[66]G. Lebedev, S. Pillet, C. Baldé, P. Guionneau, C. Desplanches, and J.-F. Létard, IOP Conf. Series: Mater. Sci. Eng. **5**, 012025 (2009).
[67]The angular distortion parameter Σ is defined as the sum of the absolute values of the deviation from 90°, of the 12 *cis* angles in the coordination sphere.
[68]M. Marchivie, P. Guionneau, J.-F. Létard, D. Chasseau, and J. A. K. Howard, J. Phys. Chem. Solids **65**, 17 (2004).
[69]T. Büchen, P. Gütlich, K. H. Sugiyarto, and H. A. Goodwin, Chem. Eur. J. **2**, 1134 (1996).
[70]N. O. Moussa, G. Molnar, S. Bonhommeau, A. Zwick, S. Mouri, K. Tanaka, J. A. Real, and A. Bousseksou, Phys. Rev. Lett. **94**, 107205 (2005).
[71]E. Trzop, M. Buron–Le Cointe, H. Cailleau, L. Toupet, G. Molnar, A. Bousseksou, A. B. Gaspar, J. A. Real, and E. Collet, J. Appl. Crystallogr. **40**, 158 (2007).
[72]E. K. H. Salje, *Phase Transitions in Ferroelastic and Co-elastic Crystals* (Cambridge University Press, Cambridge, UK, 1990).
[73]K. Boukheddaden, J. Linares, E. Codjovi, F. Varret, V. Niel, and J. A. Real, J. Appl. Phys. **93**, 7103 (2003).
[74]S. Mouri, K. Tanaka, S. Bonhommeau, N. O. Moussa, G. Molnar, and A. Bousseksou, Phys. Rev. B **78**, 174308 (2008).
[75]C. Parreira, C. Enachescu, J. Linares, K. Boukheddaden, and F. Varret, J. Phys.: Condens. Matter **12**, 9395 (2000).